

Voltammetric Determination of Dopamine at the Surface of TiO₂ Nanoparticles Modified Carbon Paste Electrode

Mohammad Mazloun-Ardakani^{1,*}, Hossein Rajabi¹, Hadi Beitollahi¹, Bi Bi Fatemah Mirjalili¹, Ali Akbari, Nima Taghavinia²

¹Department of Chemistry, Faculty of Science, Yazd University, Yazd, 89195-741, I.R. Iran

²Physics Department, Sharif University of Technology, Tehran, 14588, I.R. Iran

*E-mail: mazloun@yazduni.ac.ir

Received: 25 January 2009 / Accepted: 11 January 2009 / Published: 31 January 2010

In the present paper, the use of a novel carbon paste electrode modified by N,N'-(2,3-dihydroxybenzylidene)-1,4-phenylenediamine (DHBPD) and TiO₂ nanoparticles prepared by a simple and rapid method for the determination of dopamine (DA) was described. In the first part of the work, cyclic voltammetry was used to investigate the redox properties of this modified electrode at various solution pH values and at various scan rates. A linear segment was found with slope value of about 48 mV/pH in the pH range 2.0–12.0. The apparent charge transfer rate constant (k_s) and transfer coefficient (α) for electron transfer between DHBPD and TiO₂ nanoparticles-carbon paste electrode were calculated. In the second part of the work, the mediated oxidation of DA at the modified electrode was described. It has been found that under optimum condition in cyclic voltammetry, a high decrease in overpotential occurs for oxidation of DA at the modified electrode. The values of electron transfer coefficients (α) and diffusion coefficient (D) were calculated for DA, using electrochemical approaches. Differential pulse voltammetry (DPV) exhibited a linear dynamic range from 0.08 μ M to 20.0 μ M and a detection limit (3σ) of 3.14×10^{-8} M for DA. Finally, this method was used for the determination of DA in DA injection, using standard addition method.

Keywords: Dopamine; TiO₂ Nanoparticles; Modified carbon paste electrode; Electrocatalysis

1. INTRODUCTION

The electrochemical methods using chemically modified electrodes (CMEs) have been widely used as sensitive and selective analytical methods for the detection of the trace amounts of biologically important compounds [1-6]. One of the most important properties of CMEs has been their ability to catalyze the electrode process via significant decreasing of overpotential respect to unmodified electrodes. With respect to relatively selective interaction of the electron mediator with the target

analyte in a coordination fashion, these electrodes are capable to considerably enhance the selectivity in the electroanalytical methods.

Dopamine (DA) is an important neurotransmitter that belongs to the catecholamines group and plays a very significant role in the central nervous, renal, hormonal and cardiovascular systems [7]. Neurotransmitters (NTs) are chemical messengers that transmit a message from one neuron to the next. This transmission proceeds by secretion of the NTs from one neuron, followed by their binding to the specific receptor located on the membrane of the target cell [8]. This interaction between the NT and the receptor is one of the major ways in which neurons communicate [7]. As a result, dysfunction of the dopaminergic system in the central nervous system (CNS) has been related to neurological disorders such as schizophrenia and Parkinson's disease [9]. Thus, various commonly usable analytical methods for DA and its analogs have been developed in the past. Some examples of these methods are the rapid liquid chromatography/tandem mass spectrometry (LC-MS/MS) [10], the chromatography method [11-13], and the capillary electrophoresis mass spectrometry method [14]. These methods are very sensitive. All these techniques, however, require a compressing system, temperature controlling systems, separation systems, and other spectrophotometric or electric detection systems. In this sense, electrochemical detection of DA has received much interest due to its importance in the central nervous system (CNS). In addition, a significant problem for DA determination is the fouling effect due to accumulation of reaction products which, form electro-polymerized films on the electrode surface [15]. Thus, one promising approach to overcoming problems arising from fouling of the biological substrate is the use of chemically modified electrodes (CMEs) [16-18].

Metal, semiconductor and magnetic particles act as functional units for electroanalytical applications [19-22]. Metal nanoparticles provide three important functions for electroanalysis. These include the roughening of the conductive sensing interface, the catalytic properties of the nanoparticles permitting their enlargement with metals and the amplified electrochemical detection of the metal deposits and the conductivity properties of nanoparticles at nanoscale dimensions that allow the electrical contact of redox-centers in proteins with electrode surfaces [23]. Also, metal and semiconductor nanoparticles provide versatile labels for amplified electroanalysis [24]. Dissolution of the nanoparticles labels and the electrochemical collection of the dissolved ions on the electrode followed by the stripping-off of the deposited metals represent a general electroanalytical procedure. These unique functions of nanoparticles were employed for developing electrochemical gas sensors, electrochemical sensors based on molecular- or polymer functionalized nanoparticles sensing interfaces, and for the construction of different biosensors including immunosensors and DNA sensors [25] and enzyme based electrodes [26].

To our knowledge, no study has reported the electrocatalytic oxidation of DA by using DHBPD-TiO₂ nanoparticles modified carbon paste electrode (DHBPDTNMCPE). Thus, in the present work, we described initially the preparation and suitability of a DHBPDTNMCPE as a new electrode in the electrocatalysis and determination of DA in an aqueous buffer solution. Then, in order to demonstrate the catalytic ability of the modified electrode in the electrooxidation of DA in real samples, we examined this method for the voltammetric determination of DA in DA injection.

2. EXPERIMENTAL PART

2.1. Apparatus and chemicals

A potentiostat/galvanostat (SAMA 500, electroanalyzer system, I. R. Iran) was used for carrying out the electrochemical experiments. A conventional three electrode cell was used at $25 \pm 1^\circ\text{C}$. A saturated calomel electrode, platinum wire, and DHBPD/TNMCPE were used as reference, auxiliary and working electrodes, respectively. A Metrohm model 691 pH / mV meter was also used for pH measurements.

All solutions were freshly prepared with doubly distilled water. DA and other reagents were analytical grade (Merck, Darmstadt, Germany). Graphite powder (Merck) and paraffin oil (DC 350, Merck, density = 0.88 g cm^{-3}) were used as binding agents for graphite pastes. Buffer solutions were prepared from ortho phosphoric acid, and its salts in the pH range of 2.0–12.0.

2.2. Preparation of TiO_2 nanoparticles

Colloidal suspension of TiO_2 nanoparticles was synthesized by mixing titanium tetraisopropoxide, H_2O_2 , and H_2O with volume proportions of 12:90:200, respectively. The resulting solution was refluxed for 10 h to promote the crystallinity (surface area = $84 \text{ m}^2 \text{ g}^{-1}$ and particle size = 6.7 nm).

2.3. Typical procedure for preparation of DHBPD in the presence of 37% $\text{BF}_3 \cdot \text{SiO}_2$

A mixture of 2,3-dihydroxybenzaldehyde (0.276 g, 2.0 mmol), benzene-1,4-diamine (0.108 g, 1.0 mmol) and 37% $\text{BF}_3 \cdot \text{SiO}_2$ (0.300 g) was heated with stirring at 80°C for 15 minutes in CHCl_3 (5 mL). After completion of reaction, the product was dissolved to CHCl_3 (5 mL) and filtered to recover the catalyst. The solvent was evaporated and the crude product recrystallized from methanol compound was fully characterized by IR, ^1H NMR spectroscopy was obtained as red crystals at ~93.2% yield.

Red solid;

IR data: IR (KBr)/ σ (cm^{-1}) 3100–3300 (br, OH), 1618(s, C=N), 1407, 1506(s, Ar, C=C), 1250(s, C–O), 1218(s), 1159(s), 834, 789(s), 500(w);

NMR data: ^1H NMR(400MHz/DMSO)/ δ ppm: 3.7(br, 3H), 6.72(t, 2H), 6.91(d, 2H), 6.98(d, 2H), 7.39(s, 4H), 7.95(s, 1H), 8.7(s, 2H).

2.4. Preparation of the electrode

DHBPD/TNMCPEs were prepared by dissolving 0.01 g of DHBPD in CH_3Cl and hand mixing with 95 times its weight of graphite powder and 4 times its weight of TiO_2 nanoparticles using a mortar and pestle. Paraffin was added to the above mixture and mixed for 20 min until a uniformly wetted paste was obtained. This paste was then packed into the end of a glass tube (ca. 3.35 mm i.d. and 10

cm long). A copper wire inserted into the carbon paste provided an electrical contact. When necessary, a new surface was obtained by pushing an excess of paste out of the tube, which was then polished with weighing paper. DHBPD modified CPE (DHBPD/CPE) and TiO₂ nanoparticles CPE (TNCPE) were prepared in the same way without adding of TiO₂ nanoparticles and DHBPD respectively. Also, unmodified CPE was prepared in the same way without adding DHBPD and TiO₂ nanoparticles to the mixture. Unmodified CPEs were used for the purpose of comparison.

3. RESULTS AND DISCUSSION

3.1. Electrochemical properties of DHBPD/TNCPE

Based on our knowledge there has not been prior report of a study on the electrochemical properties and, in particular, the electrocatalytic activity of DHBPD/TNCPE in aqueous media. This compound is insoluble in aqueous media; therefore, we prepared DHBPD/TNCPE and studied its electrochemical properties in a buffered aqueous solution (pH 8.0) using cyclic voltammetry. Experimental results show well-defined and reproducible anodic and cathodic peaks (with $E_{pa} = 0.26$ V, $E_{pc} = 0.12$ V, $E^0 = 0.19$ V versus SCE and $\Delta E_p = 0.14$ V) for DHBPD, therefore this substance can be used as mediators for the electrocatalysis of some important biological compounds with slow electron transfer.

As shown, the peak separation potential, $\Delta E_p = (E_{pa} - E_{pc})$, was greater than the $59/n$ mV expected for a reversible system. This result suggests that redox couple in DHBPD/TNCPE shows quasi-reversible behavior in an aqueous medium.

In addition, the effect of the potential scan rate on electrochemical properties of the DHBPD/TNCPE was studied in an aqueous solution with cyclic voltammetry (Fig.1). Plots of the anodic and cathodic peak currents (I_p) were linearly dependent on v at scan rates from 10 to 1000 mV s⁻¹. A linear correlation was obtained between peak currents, and the scan rate indicates that the nature of redox process was controlled in a diffusionless manner (Fig. 1A).

The apparent charge transfer rate constant (k_s) and the charge transfer coefficient (α) of a surface-confined redox couple can be evaluated from cyclic voltammetric experiments and by using the variation of anodic and cathodic peak potentials with logarithm of scan rate, according to the procedure of Laviron [27]. Fig.1B shows the variations of peak potentials (E_p) as a function of the logarithm of the potential scan rate. We found that the E_p values are proportional to the logarithm of the potential scan rate, for scan rates higher than 1000 mV s⁻¹ (Fig.1B). The slopes of Fig.1B plot can be used to extract the kinetic parameters α_a (anodic transfer coefficient). The slope of the linear segment is equal to $2.303RT / (1 - \alpha) nF$ for the anodic peaks. The evaluated value for the anodic transfer coefficient (α_a) is 0.44.

Also, the following equation can be used to determine the electron transfer rate constant between modifier (DHBPD) and CPE:

$$\log k_s = \alpha \log (1-\alpha) + (1-\alpha) \log \alpha - \log (RT/nFv) - \alpha (1-\alpha) nF\Delta E_p/2.3RT \quad (1)$$

where $(1-\alpha)n_{\alpha}=0.56$, ν is the sweep rate and all other symbols having their conventional meanings. The value of $k_s = 2.36 \pm 0.13 \text{ s}^{-1}$ was evaluated using Eq. (1).

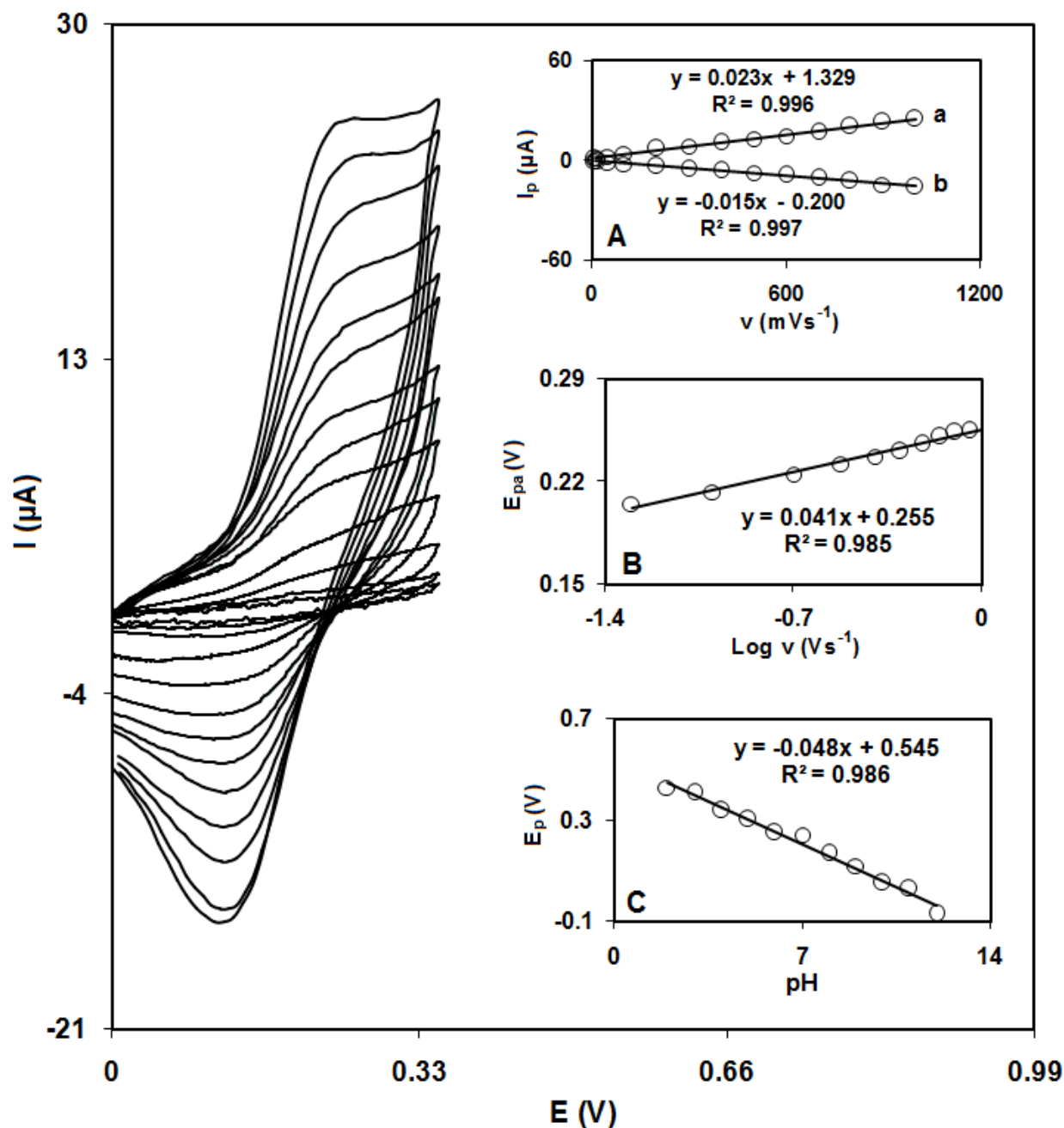


Figure 1. Cyclic voltammograms of DHBPDNTMCPE in 0.1M phosphate buffer (pH 8.0), at various scan rates, from inner to outer correspond to 10, 20, 50, 100, 200, 300, 400, 500, 600, 700, 800, 900 and 1000 mVs^{-1} scan rates, respectively. Insets: (A) Variations of I_p versus scan rates. (B) Variation of E_p versus the logarithm of the scan rate. (C) Plot of anodic potential peak (E_{pa}) of DHBPDNTMCPE vs. various pHs: 2.0, 3.0, 4.0, 5.0, 6.0, 7.0, 8.0, 9.0, 10.0, 11.0, and 12.0.

3.2. Influence of pH

The electrochemical response of the DHBPD molecule is generally pH dependent. Thus, the electrochemical behavior of the DHBPD/TNMCPE was studied at different pHs using differential pulse voltammetry. Anodic peak potentials of the DHBPD/TNMCPE were shifted to less positive values with increases in pH. A potential-pH diagram was constructed by plotting the E_p values as a function of pH (Fig. 1C). This diagram is composed of a straight line with slope = 48 mV/pH. Such behavior suggests that it obeys the Nernst equation for a two electron and proton transfer reaction [28].

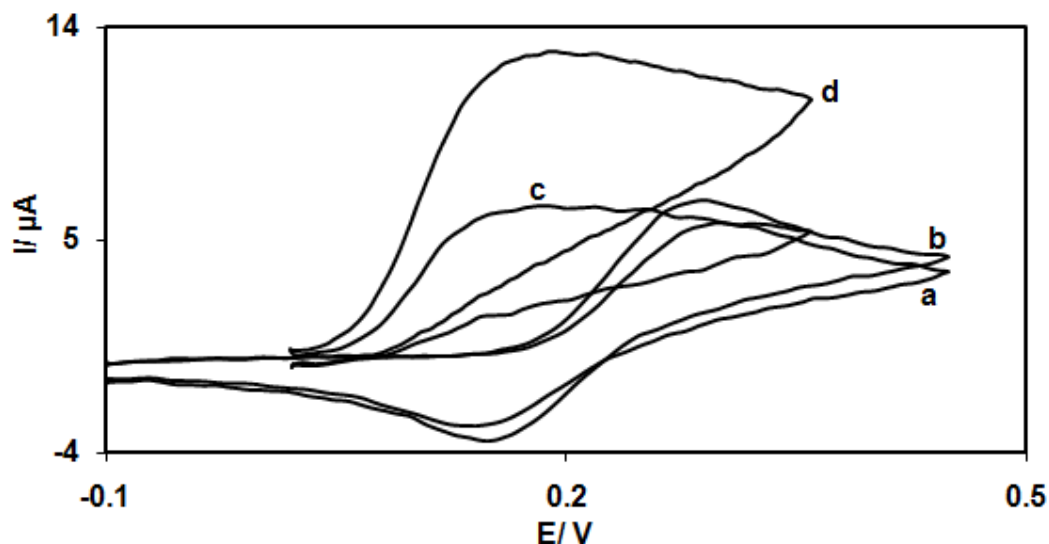


Figure 2. Cyclic voltammograms of (a) CPE and (b) TNCPE in 0.1M PBS (pH 8.0) containing 1.0 mM DA at scan rate 20 mV s^{-1} . Also, (c) and (d) as (a) at the same conditions at the surface of DHBPMCPE and DHBPD/TNMCPE respectively.

3.3. Electrocatalytic oxidation of DA at a DHBPD/TNMCPE

Fig. 2 depicts the cyclic voltammetric responses from the electrochemical oxidation of 1.0 mM DA at the unmodified CPE (curve a), TiO_2 nanoparticles CPE (TNCPE) (curve b), DHBPD modified CPE (DHBPMCPE) (curve c) and DHBPD/TNMCPE (curve d). As shown, at the DHBPMCPE (curve c) and DHBPD/TNMCPE (curve d) the peak potential were about 195 mV, while at the TiO_2 nanoparticles CPE (TNCPE) (curve b); peak potential is about 285 mV, and at the unmodified CPE (curve a) peak potential is about 310 mV for DA. From these results it is concluded that the best electrocatalytic effect for DA oxidation is observed at DHBPD/TNMCPE (curve d). For example, the results are shown that the peak potential of DA oxidation at DHBPD/TNMCPE (curve d) shifted by about 90 and 115 mV toward the negative values compared with that at a (TNCPE) (curve b) and unmodified CPE (curve a), respectively.

Similarly, when comparing the oxidation of DA at the DHBPMCPE (curve c) and DHBPD/TNMCPE (curve d), a dramatic enhancement of the anodic peak current at the

BBNBHTNMCPE relative to that obtained at the DHBPDNMCPE was observed. In other words, the data clearly show that the combination of TiO₂ nanoparticles and mediator DHBPD definitely improve the characteristics of DA oxidation.

The DHBPDNMCPE, in 0.1 M phosphate buffer (pH 8.0) at the scan rate 20 mVs⁻¹ and without DA in solution, exhibited a well-behaved redox reaction (As shown in Fig.1), upon addition of 1.0 mM DA, there was a dramatic enhancement of the anodic peak current (Fig.2 curve d), indicating a strong electrocatalytic effect [28].

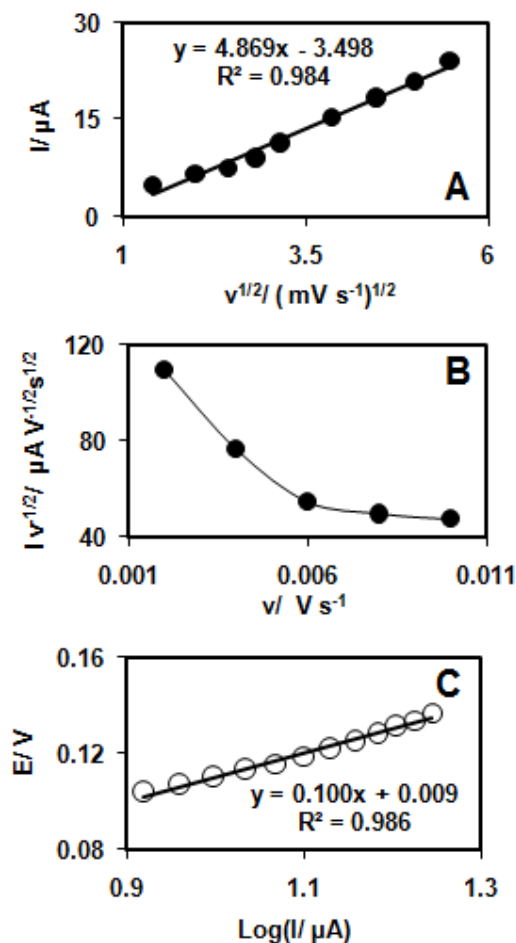


Figure 3. (A) Variation of the electrocatalytic peak current (I_p) with the square root of scan rate. Insets: (B) Variation of the scan rate-normalized current ($I_p/v^{1/2}$) with scan rate. (C) Tafel plot derived from the rising part of voltammogram recorded at a scan rate 30 mVs⁻¹.

The effect of scan rate on the electrocatalytic oxidation of DA at the DHBPDNMCPE was investigated by cyclic voltammetry. The plot of peak height (I_p) versus the square root of scan rate ($v^{1/2}$), in the range of 2–30 mV s⁻¹, was constructed (Fig. 3A). This plot was found to be linear, suggesting that, at sufficient overpotential, the process was diffusion rather than surface controlled. A plot of the sweep rate normalized current ($I_p/v^{1/2}$) versus sweep rate (Fig. 3B) exhibits the characteristic shape typical of an EC process [28].

Tafel plot was drawn from data of the rising part of the current–voltage curve recorded at a scan rate of 30 mVs^{-1} . This part of voltammogram, known as Tafel region, is affected by electron transfer kinetics between substrate (DA) and surface confined DHBPD, assuming the deprotonation of substrate as a sufficiently fast step. In this condition, the number of electron involved in the rate determining step can be estimated from the slope of Tafel plot. A slope $0.1003 \text{ Vdecade}^{-1}$ is obtained indicating a one electron transfer to be rate limiting assuming a transfer coefficient of $\alpha = 0.41$.

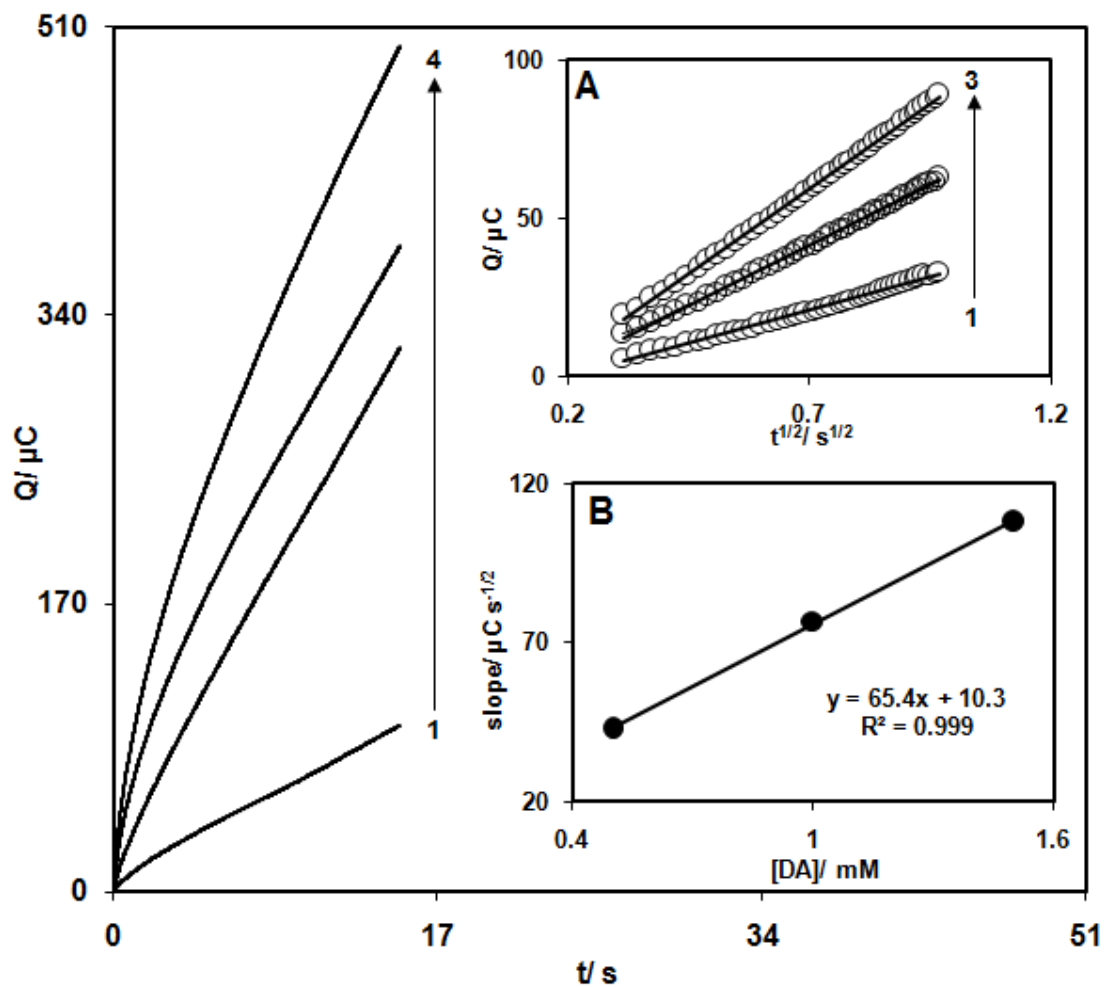


Figure 4. Chronocoulougrams obtained at DHBPD/TNMCPE in 0.1 M phosphate buffer solution (pH 8.0) for different concentration of DA by setting potential step at 280 mV. The numbers 1–4 correspond to 0.0, 0.5, 1.0 and 1.5 mM of DA. Insets: (A) Plots of Q vs. $t^{1/2}$ obtained from chronocoulougrams 2–4 and (B) plot of the slope of the straight lines against the DA concentration.

3.4. Chronocoulometric measurements

The chronocoulometry as well as the other electrochemical methods was employed for the investigation of electrode processes at chemically modified electrodes. Chronocoulometric measurements of DA at DHBPD/TNMCPE were done by setting the working electrode potential at 280

mV for various concentrations of DA (Fig.4). For an electroactive material (DA in this case) with a diffusion coefficient of D , the current for the electrochemical reaction (at a mass transport limited rate) is described by the Cottrell equation [28]. Under diffusion control, a plot of Q versus $t^{1/2}$ will be linear, and from the slope the value of D can be obtained. Fig. 4A shows the experimental plots with the best fits for different concentration of DA employed. The slopes of the resulting straight lines were plotted versus the DA concentrations (Fig. 4B). The value of the D was found to be $1.16 \times 10^{-5} \text{ cm}^2/\text{s}$.

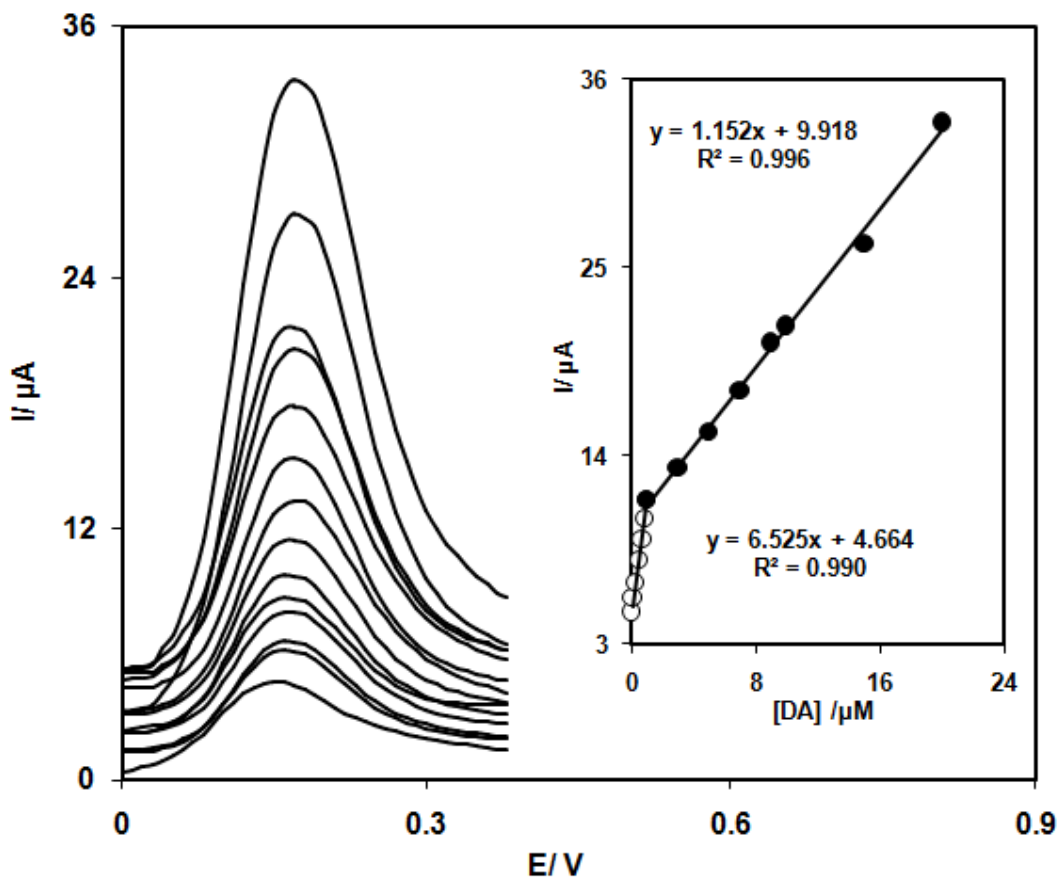


Figure 5. (A) Differential pulse voltammograms of the DHBPD TNMCPE in 0.1 M PBS (pH 8.0) containing different concentrations of DA, from inner to outer correspond to 0.08, 0.1, 0.3, 0.5, 0.7, 0.9, 1.0, 3.0, 5.0, 7.0, 9.0, 10.0, 15.0 and 20.0 μM of DA. Inset: Plot of the peak currents as a function of concentration of DA in two linear ranges of 0.08– 1.0 and 1.0 – 20.0 μM .

3.5. Calibration plot and limit of detection

Differential pulse voltammetry (DPV) was used to determine the concentration of DA. Voltammograms clearly show that the plot of peak current versus DA concentration is constituted of two linear segments with different slopes (slope: $6.525 \mu\text{A} \cdot \mu\text{M}^{-1}$ for first linear segment and $1.152 \mu\text{A} \cdot \mu\text{M}^{-1}$ for second linear segment), corresponding to two different ranges of substrate concentration, 0.08 to 1.0 μM for first linear segment and 1.0 to 20.0 μM for second linear segment. The decrease of

sensitivity (slope) in the second linear range is likely to be due to kinetic limitation. The detection limit (3σ) for DA in the lower range region was found to be 3.14×10^{-8} M.

3.6. Determination of DA in DA injection

1 mL of the DA injection solution (specified content of DA is 200 mg per 5 mL) was diluted to 50 mL with phosphate buffer, then a 10 μ L portion of the solution was diluted in a voltammetric cell to 10 mL of 0.1 M phosphate buffer (pH 8.0). I_{pa} was measured at the oxidation potential of DA by DPV. Different standard concentrations of DA were added to the diluted DA injection for testing recovery. The results are shown in Table 1.

Table 1. Determination of DA in injection samples

Sample	Original content (μ M)	Added (μ M)	Found (μ M)	Recovery (%)
1	4.2	1	5.12	98.5
2	4.2	3	7.25	100.7
3	4.2	5	9.02	98.0

4. CONCLUSIONS

This work demonstrates the construction of a DHBPDTNMCPE and its application in the determination of DA. The results showed that the oxidation of DA was catalyzed at pH 8.0, whereas the peak potential of DA was shifted by 115 mV to a less positive potential at the surface of the DHBPDTNMCPE. The catalytic peak currents obtained using DPV, were linearly dependent on the DA concentrations and the detection limit for DA was 3.14×10^{-8} M. The high current sensitivity, low detection limit and high selectivity of the DHBPDTNMCPE for the detection of DA proved its potential as a sensor.

ACKNOWLEDGEMENTS

The authors would like to thank Yazd University Research Council, IUT Research Council and Excellence in Sensors for financial support of this research.

References

1. L. Zheng, J.F. Song, *Anal. Biochem.*, 391 (2009) 56.
2. H. Beitollahi, M. Mazloum Ardakani, B. Ganjipour, H. Naeimi, *Biosens. Bioelectron.*, 24 (2008) 362.

3. M.R. Ganjali, N. Motakef-Kazami, F. Faridbod, S. Khoei, P. Norouzi, *J. Hazard. Mater.*, 173 (2010) 415.
4. M. Mazloum-Ardakani, Z. Akrami, H. Kazemian, H.R. Zare, *Int. J. Electrochem. Sci.*, 4 (2009) 308.
5. M. Mazloum Ardakani, S. M. Mirdehghan, M. M. Zare, R. Mazidi, *Sens. Actuators B*, 132 (2008) 52.
6. Z. Taleat, M. Mazloum Ardakani, H. Naeimi, H. Beitollahi, M. Nejati and H.R. Zare, *Anal. Sci.*, 24 (2008) 1039.
7. J.R. Cooper, F.E. Bloom, R.H. Roth, *The biochemical basis of neuropharmacology*, Oxford University Press, Oxford, UK, 1982.
8. D.J. Michael, R.M. Wightman, *J. Pharm. Biomed. Anal.*, 19 (1999) 33.
9. R.M. Wightman, L.J. May, A.C. Michael, *Anal. Chem.*, 60 (1988) 769.
10. M.E.P. Hows, L. Lacroix, C. Heidbreder, A.J. Organ, A.J. Shah, *J. Neurosci. Methods*, 138 (2004) 123.
11. C. Sabbioni, M.A. Saracino, R. Mandrioli, S. Pinzauti, S. Furlanetto, G. Gerra, M.A. Raggi, *J. Chromatogr. A*, 1032 (2004) 65.
12. P. Kumarathasan, R. Vincent, *J. Chromatogr. A*, 987 (2003) 349.
13. M. Tsunoda, C. Aoyama, H. Nomura, T. Toyoda, N. Matsuki, T. Funatsu, *J. Pharm. Biomed. Anal.*, 51 (2010) 712.
14. Z.D. Peterson, D.C. Collins, C.R. Bowerbank, M.L. Lee, S.W. Graves, *J. Chromatogr. B*, 776 (2002) 221.
15. R.F. Lane, C.D. Blaha, *Longmuir*, 6 (1990) 56.
16. M. Mazloum-Ardakani, H. Beitollahi, B. Ganjipour, H. Naeimi, M. Nejati, *Bioelectrochemistry* 75 (2009) 1.
17. J.G. Manjunatha, B.E. Kumara S.G.P. Mamatha, U. Chandra, E. Niranjana, B.S. Sherigara, *Int. J. Electrochem. Sci.*, 4 (2009) 187.
18. M. Mazloum Ardakani, A. Talebi, H. Naeimi, M. Nejati Barzoky, N. Taghavinia, *J. Solid State Electrochem.*, 13 (2009) 1433.
19. C. Ozdemir, F. Yeni, D. Odaci, S. Timur, *Food Chem.*, 119 (2010) 380.
20. M. Mazloum Ardakani, Z. Taleat, H. Beitollahi, M. Salavati-Niasari, B.B.F. Mirjalili, N. Taghavinia, *J. Electroanal. Chem.*, 624 (2008) 73.
21. L. Zhang, Z. Fang, G.C. Zhao, X.W. Wei, *Int. J. Electrochem. Sci.*, 3 (2008) 746.
22. H.J. Wang, C.M. Zhou, F. Peng, H. Yu, *Int. J. Electrochem. Sci.*, 2 (2007) 508.
23. N. Zheng, X. Zhou, W. Yang, X. Li, Z. Yuan, *Talanta*, 79 (2009) 780.
24. S. Jingyu, H. Jianshu, C. Yanxia, Z. Xiaogang, *Int. J. Electrochem. Sci.*, 2 (2007) 64.
25. H. Gao, J. Zhong, P. Qin, C. Lin, W. Sun, *Microchem. J.*, 93 (2009) 78.
26. K. Can, M. Ozmen, M. Ersoz, *Colloids Surf. B*, 71 (2009) 154.
27. E. Laviron, *J. Electroanal. Chem.*, 101(1979)19.
28. A.J. Bard, L.R. Faulkner, *Electrochemical Methods: Fundamentals and Applications*, second ed., Wiley, New York, 2001.